

On continuous deformations of monohedral spherical tilings by spherical pentagons

Ana Maria Reis d'Azevedo Breda
Departamento de Matemática
Universidade de Aveiro
Aveiro, Portugal
ambreda@ua.pt

José Manuel Dos Santos Dos Santos
Instituto GeoGebra Portugal
Escola Superior de Educação - Politécnico do Porto
Porto, Portugal
santosdosantos@ese.ipp.pt

Abstract—In a previous work it was described a procedure to obtain certain classes of spherical tilings with GeoGebra, starting from a specific subset of spherical segments. This innovative way of generating spherical tilings has made emerged a class of monohedral spherical tiling by four spherical pentagons and classes of dihedral spherical tiling by twelve spherical pentagons. Here, we shall show how we can generate a class of a 2-parameter monohedral spherical tilings by convex pentagons, $\mathfrak{T}_{(\mathcal{G}, \theta_1, \theta_2)}^*$, made of sixty congruent tiles, changing the gluing rules of the edge-tiles, being the new ones ruled by a local action of a particular subgroup of spherical isometries with support on the regular spherical dodecahedral tiling. In relation to these new classes of pentagonal tilings, combinatorial and geometric properties will be given. All monohedral spherical tilings by pentagons whose pentagonal prototile is of the form $a.a.b.b.c$ are shown. This family of spherical tilings has emerged as a result of an interactive construction process using newly produced GeoGebra tools and the dynamic interaction capabilities of this software.

Index Terms—Spherical Geometry, Spherical Tilings, GeoGebra.

I. INTRODUCTION

By a spherical tiling we mean a tiling of the 2-dimensional sphere [13]. A spherical tiling is monohedral if all tiles are congruent. Additionally, a spherical tiling is edge-to-edge if no vertex of a tile lies in the interior of an edge of another tile. In this paper we are interested in the study of new classes of monohedral and edge-to-edge spherical tilings by spherical pentagons.

The spherical tilings by congruent right triangles were obtained by Yukako Ueno and Yoshio Agaoka in 1996, [22]. Later, in 2002, the complete classification of monohedral edge-to-edge triangular spherical tilings was achieved by the same authors [23]. They have extended the classification of triangular f-spherical foldings, studied and characterised by Ana Breda, in 1992, [1].

The classification of spherical tilings by triangles is not yet completed. In fact, little is known when the condition of being monohedral or edge-to-edge is dropped out.

The combinatorial study of spherical tilings by twelve pentagons, with vertex valency greater or equal to three has been also achieved, see [12] for details. Recently, a family of spherical monohedral tiling by four congruent and non-convex spherical pentagons has been characterised [7].

Besides the theoretical mathematical aspects involved in the study of spherical tilings, they are also object of interest in other areas of knowledge and in technological applications. Walter Kohn pointed the year 1984 as the year where a big surprise in the field of crystallography has occurred. In [15, p. s70] he mentions: “D. Schechtman and co-workers that reported a beautiful x-ray pattern with unequivocal icosahedral symmetry for rapidly quenched AlMn compounds. The appropriate theory was independently developed by D. Levine and P. Steinhardt, who coined the words quasicrystal and quasiperiodic. Even more curious was the fact that R. Penrose (1984) had anticipated these concepts in purely geometric [terms], the so-called Penrose tilings” [15, p. s70].

Spherical tilings and their properties have been used in chemistry, for instance, in the study of periodic nanostructures [11], making emerge new forms of molecular association notably fullerenes [10], leading to a deeper study of spherical tilings by triangles, quadrilaterals and pentagons [19]. In the same line of reasoning other tilings including heptagons [21], and, heptagons and octagons [20] had emerged. Applications to new possibilities for new molecular patterns are exposed in [8], [14], [17], [18], [24]. Nowadays, in engineering there is a need to merge the computer aided design and computer aided engineering into a single approach, contributing to an increasing interest in studying relationships between spherical tilings and spherical Bezier curves [9]. The knowledge of spherical tilings can also be useful for the developed of some issues in computational algebra [16]. The facility location problems, spherical designs and minimal energy point configurations on spheres [2], [3] are other fields where the study of spherical tilings is quite useful.

In this paper we intend to extend the knowledge of spherical tilings describing a set of spherical tilings, here denoted by \mathfrak{T} , presenting and characterising, in detail, some subsets of \mathfrak{T} composed by pentagonal monohedral spherical tilings with sixty tiles, providing a continuous deformation path among elements of this class. We also present a way to obtain all monohedral spherical tilings by convex spherical pentagons whose their tile configurations are of the type $a.a.b.b.c$.

II. RELATED WORK

In previous work, making use of the dynamic capabilities of GeoGebra, that have been proved to be interesting for our research, findings about monohedral and dihedral spherical tilings by spherical convex and non convex pentagons were obtained.

The creation of GeoGebra tools for spherical geometry, used initially to obtain some well known spherical tilings, provide geometric concretization of some new spherical tilings [6].

In fact, GeoGebra gives the possibility of interacting, simultaneously, with graphic, algebraic and calculus views. It also gives the chance to create new tools and commands. All tools was created from the combination of existing tools or commands. The new tool and the corresponding commands can be used in new constructions or may be integrated in the construction of new tools. Spherical GeoGebra tools were constructed among the purpose to explore, among others spherical tilings. Whiting these spherical tools we mention the following ones: *Spherical Segment, Minor, Spherical Segment, Great, SphericalAngleMeasure, Spherical Equidistant Points, Spherical Compass, Spherical Equilateral Triangle, SphericalTriangleVertice3Angles, SphericalTriangle β AB α* .

Here, by way of example, we describe how the Spherical Segment tool was constructed.

Given two non antipodal spherical points A and B, the minor spherical segment joining them is a great circular arc of extremes A and B. These spherical segment can be obtained in GeoGebra using the command *SphereSegmentMinor*[A,B] described below (see figure 1).


Tool Name	Spherical Segment, minor
Command Name	SphericalSegmentMinor
Syntax	SphericalSegmentMinor[A,B]
Help	Given A,B and a spherical, s, draw the spherical segment joining A to B.
Icon	
Script	s=Sphere[(0,0,0), 1] A=PointIn[s] B=PointIn[s] If[Distance[A,B]≠2,CircularArc[(0,0,0), A,B,Plane[(0,0,0),A,B]]]

Figure 1: Construction of the spherical segment minor tool

Observed that if we use, in the the last line of the script of figure 1, the command *Plane*[(0,0,0),B,A] we get the greater spherical segment between two points and, by these way, we can record a different tool.

These new tools allowed us to get new families of spherical tilings, namely, the 2-parameter family, \mathfrak{B}_q^p , $p, q \in \mathbb{N}$, obtained by a global action of a subgroup of spherical isometries, which contains the well known antiprismatic tilings see [5]. Later, using similar procedures, the one-parameter family of tilings, $\mathfrak{P}_{(\mathcal{C},\tau)}$ with $\tau \in]0, \pi[\setminus \{ \frac{1}{2} \arccos(-\frac{1}{3}) \}$, was revealed, see [7]. Recently, the one-parameter family of monohedral spherical non-convex hexagonal tiling with six faces, $\mathfrak{H}_{(\mathcal{C},\tau)}$, $\tau \in]0, \arcsin(\frac{\sqrt{6}}{3}) + \frac{\pi}{2} [\setminus \{ \arctan(\frac{\sqrt{2}}{2}) \}$ was described [4].

As we shall see, in the next sections, an adequate adaptation of the previous procedures permit us to characterise a 2-

parameter class of monohedral spherical tiling composed of sixty congruent pentagonal tiles, $\mathfrak{P}_{(\mathcal{C},\theta_1,\theta_2)}^*$, with parameters $\theta_1 \in [0, \arccos(l_1)]$ and $\theta_2 \in [0, \arccos(l_2)]$ where

$$l_1 = \frac{1}{10} \sqrt{10(\sqrt{5}+5)}$$

and

$$l_2 = \frac{\alpha \left((4-2\sqrt{5})\beta - \sqrt{2} \sqrt{(4\beta^2-3)(\sqrt{5}-3)} \right)}{3(\sqrt{5}-3)} + \beta^2$$

with $\alpha = \cos(\theta_1)$ and $\beta = \sin(\theta_1)$.

III. CONSTRUCTION OF \mathcal{C} , THE TILING GENERATION CELL.

Consider one of the pentagonal tiles, $[ABCDE]$, of the regular dodecahedral spherical tiling. Without loss of generality we may assume that the equilateral spherical pentagon $[ABCDE]$ of angles $\frac{2\pi}{3}$, has as vertices the points A, B, C, D, E whose coordinates are:

$$A = \left(\frac{\sqrt{15}+\sqrt{3}}{6}, -\frac{\sqrt{15}+\sqrt{3}}{6}, 0 \right); \quad B = \left(\frac{\sqrt{15}+\sqrt{3}}{6}, \frac{\sqrt{15}-\sqrt{3}}{6}, 0 \right);$$

$$C = \left(\frac{\sqrt{3}}{3}, \frac{\sqrt{3}}{3}, \frac{\sqrt{3}}{3} \right); \quad D = \left(\frac{\sqrt{15}-\sqrt{3}}{6}, 0, \frac{\sqrt{15}+\sqrt{3}}{6} \right);$$

$$E = \left(\frac{\sqrt{3}}{3}, -\frac{\sqrt{3}}{3}, \frac{\sqrt{3}}{3} \right).$$

The centroid of the prototile is the point

$$C_t = \left(\frac{\sqrt{10}\sqrt{5}+50}{10}, 0, \frac{\sqrt{-10}\sqrt{5}+50}{10} \right)$$

and the coordinates of the midpoint of the geodesic joining the spherical points A and B is $M_{AB} = (1, 0, 0)$. It should be noted that C_t is determined by the intersection of the geodesic segments $M_{AB}D$ and AM_{CD} where $M_{CD} = \left(\frac{1}{2}, \frac{\sqrt{5}-1}{4}, \frac{\sqrt{5}+1}{4} \right)$.

The side lengths of the spherical triangle $[AM_{AB}C_t]$ are:

$$\widehat{AM_{AB}} = \arccos\left(\frac{\sqrt{3}+\sqrt{15}}{6}\right);$$

$$\widehat{M_{AB}C_t} = \arccos\left(\frac{1}{10}\sqrt{10(\sqrt{5}+5)}\right);$$

$$\widehat{C_tA} = \arccos\left(\frac{\sqrt{15(2\sqrt{5}+5)}}{15}\right).$$

Having in mind the use of an adaption to the procedure performed in previous work and using the dynamic displacement of a point P in the region defined by the spherical triangle $[AM_{AB}C_t]$, we end up, as we shall see, with a class of pentagonal tilings. In fact, some elements of this class are monohedral tilings by triangles and quadrilaterals. They are limit cases of the pentagonal ones, see Fig.2.

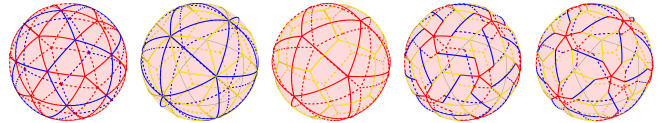


Figure 2: Some elements of $\mathfrak{P}_{(\mathcal{C},\theta_1,\theta_2)}^*$, monohedral spherical tilings by triangles, kites, quadrilaterals and pentagons.

Consider the set $\mathcal{C} = \{X \in S^2 : X \in \widehat{PA} \vee X \in \widehat{PM_{AB}} \vee X \in \widehat{PC_t}\}$, $P \in [AM_{AB}C_t]$, which represents the starting cell of the generating tilings. In Figure 3, we illustrate a tiling obtained through the generating procedure described bellow, with θ_1, θ_2 the midpoints of the corresponding admissible intervals.

Let θ_1 be an angle in $[0, l_1]$. To obtain a dynamic variation of P in all points of the fundamental region, $[AM_{AB}C_t]$, let us

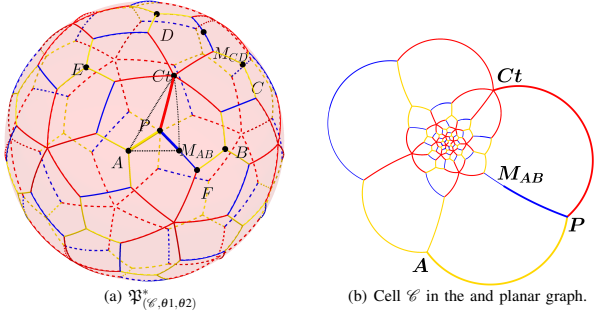


Figure 3: Element of the monohedral spherical tiling family $\mathfrak{P}_{(\mathcal{C}, \theta_1, \theta_2)}^*$ and one of its planar graph.

take an arbitrary point $X_{\theta_1} \in \widehat{OM_{AB}Ct}$ and consider the point \hat{X}_{θ_2} obtained by the intersection of the plane $z = \sin \theta_1$ with the spherical segment \widehat{ACt} . Let P be an arbitrary point in the spherical segment $\widehat{X_{\theta_1}\hat{X}_{\theta_2}}$. Denoted by θ_2 the $\widehat{X_{\theta_1}P}$, see figure 4.

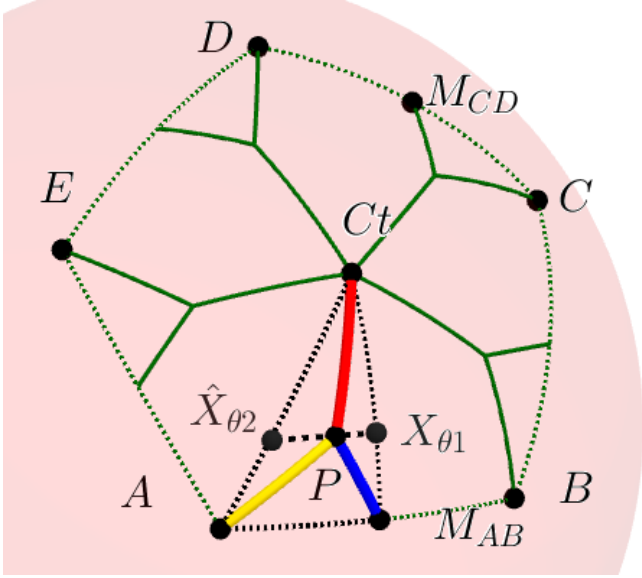


Figure 4: Detail of construction of P in \mathcal{C} of $\mathfrak{P}_{(\mathcal{C}, \theta_1, \theta_2)}^*$.

Thus, P is in the intersection of the planes $OM_{AB}Ct$ and $z = \sin \theta_1$ with the sphere. Consequently, the coordinates of P fulfil the equations: $x^2 + y^2 + z^2 = 1$; $z = \sin \theta_1$; $-\frac{1}{15}x\sqrt{15(-2\sqrt{5}+5)} - \frac{1}{30}y\sqrt{30(\sqrt{5}+5)} + \frac{1}{30}z\sqrt{30(-\sqrt{5}+5)} = 0$; leading to $\frac{1}{2}\sin \theta_1^2(-\sqrt{5}+5) + \frac{1}{2}x^2(-3\sqrt{5}+9) + \sin \theta_1 x(-2\sqrt{5}+4) - 1 = 0$, which mean that $\theta_1 \in \left[-\frac{1}{2}\arccos\left(\frac{\sqrt{5}-10}{15}\right), \frac{1}{2}\arccos\left(\frac{\sqrt{5}-10}{15}\right)\right]$.

Having in account the definition of \hat{X}_{θ_2} , we may conclude that its coordinates are:

$$\frac{-\sqrt{2}\sqrt{(\sqrt{5}-3)(4\sin^2(\theta_2)-3)}-2\sqrt{5}\sin(\theta_2)+4\sin(\theta_2)}{3(\sqrt{5}-3)};$$

$$\frac{-\sqrt{2}\sqrt{(\sqrt{5}-3)(4\sin^2(\theta_2)-3)}+\sqrt{5}\sin(\theta_2)+\sin(\theta_2)}{6};$$

and $\sin(\theta_2)$, respectively.

Accordingly, $(\cos(\theta_1)\cos(-\theta_2), \cos(\theta_1)\sin(-\theta_2), \sin(\theta_1))$ was the coordinates of point P , that is one of the vertices of the generated tiling.

IV. FROM \mathcal{C} TO THE $\mathfrak{P}_{(\mathcal{C}, \theta_1, \theta_2)}^*$

Let us consider the set of the following eighth spherical rotations:

$$\mathcal{I} = \left\{ \left(\mathcal{R}_{(Ct, k\frac{2\pi}{5})} \right)_{k \in \{1, \dots, 4\}}, \mathcal{R}_{(M_{AB}, \pi)}, \mathcal{R}_{(A, \frac{4\pi}{3})}, \mathcal{R}_{(A_2, \frac{2\pi}{3})}, \mathcal{R}_{(C, \frac{2\pi}{3})} \right\},$$

where:

$$A_2 = \mathcal{R}_{(A, \frac{2\pi}{5})}(\mathcal{R}_{(M_{AB}, \pi)}(Ct)) = \left(\frac{\sqrt{3}}{3}, -\frac{\sqrt{3}}{3}, -\frac{\sqrt{3}}{3} \right).$$

The matricial representation of the elements of \mathcal{I} are:

$$\mathcal{R}_{(Ct, \frac{2\pi}{5})} = \begin{pmatrix} \frac{\sqrt{5}+1}{4} & -\frac{1}{2} & \frac{\sqrt{5}-1}{4} \\ \frac{1}{2} & \frac{\sqrt{5}-1}{4} & -\frac{\sqrt{5}-1}{4} \\ \frac{\sqrt{5}-1}{4} & \frac{\sqrt{5}+1}{4} & \frac{1}{2} \end{pmatrix};$$

$$\mathcal{R}_{(Ct, \frac{4\pi}{5})} = \begin{pmatrix} \frac{1}{2} & -\frac{\sqrt{5}+1}{4} & \frac{\sqrt{5}+1}{4} \\ \frac{\sqrt{5}-1}{4} & -\frac{\sqrt{5}-1}{4} & -\frac{1}{2} \\ \frac{\sqrt{5}+1}{4} & \frac{1}{2} & -\frac{\sqrt{5}+1}{4} \end{pmatrix};$$

$$\mathcal{R}_{(Ct, \frac{6\pi}{5})} = \begin{pmatrix} \frac{1}{2} & \frac{\sqrt{5}-1}{4} & \frac{\sqrt{5}+1}{4} \\ -\frac{\sqrt{5}+1}{4} & -\frac{\sqrt{5}-1}{4} & \frac{1}{2} \\ \frac{\sqrt{5}+1}{4} & -\frac{1}{2} & -\frac{\sqrt{5}+1}{4} \end{pmatrix};$$

$$\mathcal{R}_{(Ct, \frac{8\pi}{5})} = \begin{pmatrix} \frac{\sqrt{5}+1}{4} & \frac{1}{2} & \frac{\sqrt{5}-1}{4} \\ -\frac{1}{2} & \frac{\sqrt{5}-1}{4} & \frac{\sqrt{5}+1}{4} \\ \frac{\sqrt{5}-1}{4} & -\frac{\sqrt{5}-1}{4} & \frac{1}{2} \end{pmatrix};$$

$$\mathcal{R}_{(A, \frac{4\pi}{3})} = \begin{pmatrix} \frac{\sqrt{5}+1}{4} & -\frac{\sqrt{5}-3}{4} & \frac{\sqrt{5}+1}{4} \\ -\frac{\sqrt{5}-3}{4} & \frac{\sqrt{5}+1}{4} & \frac{\sqrt{5}+1}{4} \\ -\frac{\sqrt{5}-1}{4} & -\frac{\sqrt{5}-1}{4} & -\frac{1}{2} \end{pmatrix};$$

$$\mathcal{R}_{(M_{AB}, \pi)} = \begin{pmatrix} 1 & 0 & 0 \\ 0 & -1 & 0 \\ 0 & 0 & -1 \end{pmatrix};$$

$$\mathcal{R}_{(A_2, \frac{2\pi}{3})} = \begin{pmatrix} 0 & 1 & 0 \\ 0 & 0 & -1 \\ -1 & 0 & 0 \end{pmatrix};$$

$$\mathcal{R}_{(C, \frac{2\pi}{3})} = \begin{pmatrix} 0 & 0 & 1 \\ 1 & 0 & 0 \\ 0 & 1 & 0 \end{pmatrix}.$$

Consider:

$$\mathcal{C}^0 = \mathcal{C} \text{ (graphically represented in figure 3(b)),}$$

$$\mathcal{C}^1 = \bigcup_{i=1}^4 \mathcal{R}_{(Ct, i\frac{2\pi}{5})}(\mathcal{C}^0),$$

$$\mathcal{C}^2 = \mathcal{R}_{(M_{AB}, \pi)}(\mathcal{C}^1),$$

$$\mathcal{C}^3 = \mathcal{R}_{(A, \frac{4\pi}{3})}(\mathcal{C}^2),$$

$$\mathcal{C}^4 = \mathcal{R}_{(A_2, \frac{2\pi}{3})}(\mathcal{C}^3),$$

$$\mathcal{C}^5 = \mathcal{R}_{(C, \frac{2\pi}{3})}(\bigcup_{i=1}^4 \mathcal{C}^i) \text{ and}$$

$$\mathcal{C}^6 = \mathcal{R}_{(C, \frac{2\pi}{3})}(\mathcal{C}^5).$$

Under these conditions the set $\bigcup_{i=0}^6 \mathcal{C}^i$ define the spherical class of tilings $\mathfrak{P}_{(\mathcal{C}, \theta_1, \theta_2)}^*$.

Besides each tile has internal angles of the form $(\frac{2\pi}{3}, *i, \frac{2\pi}{5}, *i, *i)$, where the $*i$, $i \in \{1, 2, 3\}$, are uniquely determined for each value of θ_1, θ_2 .

The pentagonal tilings in $\mathfrak{P}_{(\mathcal{C}, \theta_1, \theta_2)}^*$ are composed by sixty pentagonal congruent tiles, and so the sum of the internal angles of each tile is $\frac{13\pi}{5}$.

Thus, given the coordinates of the points A, P, M_{AB} and C_t , we may compute the angle measure defined by them:

$$\begin{aligned} \cos(\widehat{APM_{AB}}) &= \frac{1}{12} (\sin(\theta_1 + \theta_2) - \sin(\theta_1 - \theta_2)) \\ &\quad ((\cos(\theta_1) \cos(\theta_2) (-\sqrt{3} + \sqrt{15}) \\ &\quad + \cos(\theta_1) \sin(\theta_2) (-\sqrt{3} - \sqrt{15})) \\ &\quad + \frac{1}{6} \sin^2(\theta_1) (-\sqrt{3} - \sqrt{15})); \\ \cos(\widehat{M_{AB}PC_t}) &= -\frac{1}{10} \cos(\theta_1)^2 \sin(\theta_2)^2 \sqrt{10(\sqrt{5} + 5)} \\ &\quad - \frac{1}{10} \sin(\theta_1)^2 \sqrt{10(\sqrt{5} + 5)} \\ &\quad + \cos(\theta_1) \cos(\theta_2) \sin(\theta_1) \frac{1}{10} \sqrt{10(-\sqrt{5} + 5)}; \\ \cos(\widehat{C_tPA}) &= -\frac{1}{15} \cos(\theta_1)^2 \sin(\theta_2)^2 \sqrt{15(2\sqrt{5} + 5)} \\ &\quad - \frac{1}{15} \sin(\theta_1)^2 \sqrt{15(2\sqrt{5} + 5)} + \cos(\theta_1) \cos(\theta_2) \sin(\theta_1) \times \\ &\quad \frac{1}{30} \sqrt{30(\sqrt{5} + 5)} + \cos(\theta_1) \sin(\theta_1) \sin(\theta_2) \times \\ &\quad \frac{1}{15} \sqrt{15(-2\sqrt{5} + 5)} + \cos(\theta_1)^2 \cos(\theta_2) \sin(\theta_2) \times \\ &\quad \frac{1}{30} \sqrt{30(-\sqrt{5} + 5)}, \end{aligned}$$

and so all the internal angle measure of the tile are known.

The dynamic process described above allow us to characterise all the elements of the family $\mathfrak{P}_{(\mathcal{C}, \theta_1, \theta_2)}^*$. First, we note that there are elements in this family which do not correspond to pentagonal spherical tilings. In fact, only angles, θ_1 and θ_2 , taken in the interior of their admissibility intervals correspond to pentagonal monohedral tilings, being these composed by sixty spherical tiles (as we can see one example in Fig. 3(a)). The remaining cases correspond to monohedral spherical tilings by triangles and quadrilaterals.

The elements of $\mathfrak{P}_{(\mathcal{C}, \theta_1, \theta_2)}^*$ with $\theta_1 \in]0, l_1[$ and $\theta_2 \in]0, l_2[$ belong to a family of a two parameter not yet described in the literature.

Any element of this family is composed by sixty 60 spherical pentagons, with 150 edges and 92 vertices, 12 of them of valence 5 and the others 80 vertices of valence 3, and have the tile configuration $y.y.r.r.(2b)$.

The process here described can be applied generate spherical tilings supported in the others regular spherical tilings, i.e, tetrahedral, \mathcal{T} ; hexahedral, \mathcal{H} ; octahedral, \mathcal{O} ; and icosahedral, \mathcal{I} .

We get three monohedral spherical tilings by pentagon, $\mathfrak{P}_{(\mathcal{C}_{\mathcal{H}}, \theta_1^{\mathcal{H}}, \theta_2^{\mathcal{H}})}^*$ where $\mathcal{H} \in \{\mathcal{T}, \mathcal{H}, \mathcal{O}, \mathcal{I}\}$. For each $\mathcal{C}_{\mathcal{H}}$, we proceed changing the gluing rules of the edge-tiles according a local action of particular subgroups of spherical isometries related with the corresponding regular \mathcal{H} spherical tiling. It should be note that: $\mathfrak{P}_{(\mathcal{C}_{\mathcal{O}}, \theta_1^{\mathcal{O}}, \theta_2^{\mathcal{O}})}^*$ and $\mathfrak{P}_{(\mathcal{C}_{\mathcal{I}}, \theta_1^{\mathcal{I}}, \theta_2^{\mathcal{I}})}^*$ defines the same families of tilings; $\mathfrak{P}_{(\mathcal{C}_{\mathcal{H}}, \theta_1^{\mathcal{H}}, \theta_2^{\mathcal{H}})}^*$ and $\mathfrak{P}_{(\mathcal{C}_{\mathcal{O}}, \theta_1^{\mathcal{O}}, \theta_2^{\mathcal{O}})}^*$ defines the same families of tilings .

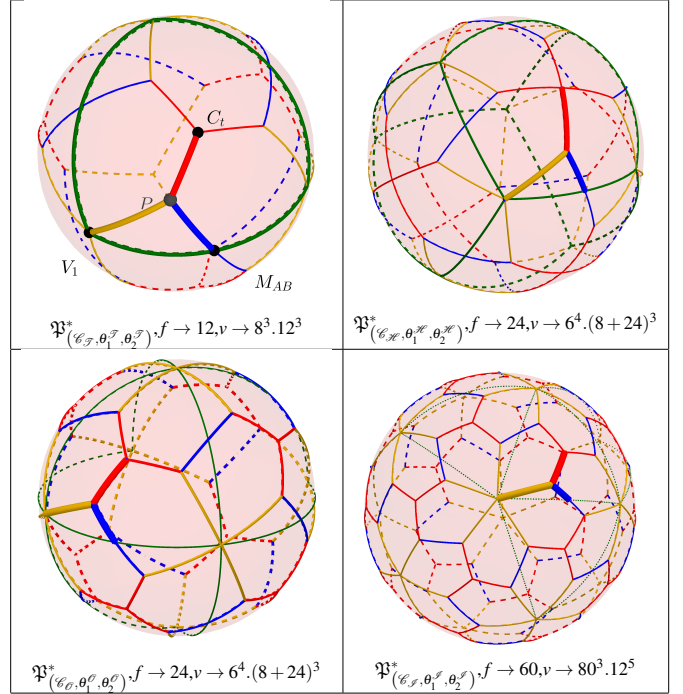


Figure 5: Elements of $\mathfrak{P}_{(\mathcal{C}_{\mathcal{H}}, \theta_1^{\mathcal{H}}, \theta_2^{\mathcal{H}})}^*$, $\mathcal{H} \in \{\mathcal{T}, \mathcal{H}, \mathcal{O}, \mathcal{I}\}$.

These procedures led to the characterisation of three class of monohedral pentagonal spherical tilings, where all the tilings have the tile configuration $y.y.r.r.(2b)$, whose some geometrical and combinatorial characterisation are specified in figure 5.

V. CONCLUSION

Here, we have shown how a suitable adaptation of a procedure for generating spherical tilings starting from a cell, composed by three spherical arcs, and described in previous work, with support in the regular dodecahedral spherical tiling, led to a two parameter family of pentagonal monohedral tiling of the sphere with sixty faces. This approach was possible by mean of computational tools. We also show some of the results of the adaptation of the procedure here described in order to present all the monohedral pentagonal tiling with the tile configuration $y.y.r.r.(2b)$. Next step will be the detailed description of these new pentagonal tilings.

This work highlights the potential of the geometric approach supported by a dynamic geometry software for the search and analysis of spherical tilings, revealing connections that a combinatorial approach would not have.

ACKNOWLEDGMENT

This research was supported by the Portuguese national funding agency for science, research and technology (FCT), within the Center for Research and Development in Mathematics and Applications (CIDMA), project UID/MAT/04106/2019.

REFERENCES

- [1] Ana M. R. Azevedo Breda. A class of tilings of s^2 . *Geometriae Dedicata*, 44(3):241–253, Dec 1992.
- [2] Carlos Beltrán. A facility location formulation for stable polynomials and elliptic feketete points. *Foundations of Computational Mathematics*, 15(1):125–157, 2015.
- [3] Johann S Brauchart and Peter J Grabner. Distributing many points on spheres: minimal energy and designs. *Journal of Complexity*, 31(3):293–326, 2015.
- [4] Ana Maria D’Azevedo Breda and José Manuel Dos Santos Dos Santos. New classes of monohedral spherical tilings by non-convex spherical hexagons and non-convex spherical pentagons with geogebra. In Gordon Lee and Ying Jin, editors, *Proceedings of 34th International Conference on Computers and Their Applications*, volume 58 of *EPiC Series in Computing*, pages 75–82. EasyChair, 2019.
- [5] Ana M d’Azevedo Breda and José M Dos Santos Dos Santos. Spherical geometry and spherical tilings with geogebra. *Journal for Geometry and Graphics*, 22(2):283–299, 2018.
- [6] Ana M d’Azevedo Breda and José M Dos Santos Dos Santos. Spherical tiling with geogebra - new results, challenges and open problems. 2019in press.
- [7] Ana M d’Azevedo Breda and José M Dos Santos Dos Santos. A new class of monohedral pentagonal spherical tilings with geogebra. *Portugaliae Mathematica*, 74(3):257–266, 2018.
- [8] Bart De Nijs, Simone Dussi, Frank Smalenburg, Johannes D Meeldijk, Dirk J Groenendijk, Laura Filion, Arnout Imhof, Alfons Van Blaaderen, and Marjolein Dijkstra. Entropy-driven formation of large icosahedral colloidal clusters by spherical confinement. *Nature materials*, 14(1):56, 2015.
- [9] Sander Dedoncker, Laurens Coox, Florian Maurin, Francesco Greco, and Wim Desmet. Bézier tilings of the sphere and their applications in benchmarking multipatch isogeometric methods. *Computer Methods in Applied Mechanics and Engineering*, 332:255 – 279, 2018.
- [10] Michel Deza, Patrick W Fowler, A Rassat, and Kevin M Rogers. Fullerenes as tilings of surfaces. *Journal of chemical information and computer sciences*, 40(3):550–558, 2000.
- [11] Mircea V Diudea and Csaba L Nagy. *Periodic nanostructures*, volume 7. Springer Science & Business Media, 2007.
- [12] Honghao Gao, Nan Shi, and Min Yan. Spherical tiling by 12 congruent pentagons. *Journal of Combinatorial Theory, Series A*, 120(4):744 – 776, 2013.
- [13] Branko Grünbaum and Geoffrey Colin Shephard. *Tilings and patterns*. Freeman, New York, 1987.
- [14] Giuliana Indelicato, Newton Wahome, Philippe Ringler, Shirley A. Müller, Mu-Ping Nieh, Peter Burkhard, and Reidun Twarock. Principles governing the self-assembly of coiled-coil protein nanoparticles. *Biophysical Journal*, 110(3):646 – 660, 2016.
- [15] Walter Kohn. An essay on condensed matter physics in the twentieth century. *Reviews of Modern Physics*, 71(2):S59, 1999.
- [16] Joachim König, Arielle Leitner, and Danny Neftin. Almost-regular dessins d’enfant on a torus and sphere. *Topology and its Applications*, 243:78 – 99, 2018.
- [17] Majid Mosayebi, Deborah K. Shoemark, Jordan M. Fletcher, Richard B. Sessions, Noah Linden, Derek N. Woolfson, and Tanniemola B. Liverpool. Beyond icosahedral symmetry in packings of proteins in spherical shells. *Proceedings of the National Academy of Sciences*, 114(34):9014–9019, 2017.
- [18] Manica Negahdaripour, Nasim Golkar, Nasim Hajighahramani, Sedigheh Kianpour, Navid Nezafat, and Younes Ghasemi. Harnessing self-assembled peptide nanoparticles in epitope vaccine design. *Biotechnology Advances*, 35(5):575 – 596, 2017.
- [19] Ali Asghar Rezaei. Polygonal tiling of some surfaces containing fullerene molecules. *Iranian Journal of Mathematical Chemistry*, 5(2):99–105, 2014.
- [20] Ali Asghar Rezaei. Tiling fullerene surface with heptagon and octagon. *Fullerenes, Nanotubes and Carbon Nanostructures*, 23(12):1033–1036, 2015.
- [21] Yuan-Zhi Tan, Rui-Ting Chen, Zhao-Jiang Liao, Jia Li, Feng Zhu, Xin Lu, Su-Yuan Xie, Jun Li, Rong-Bin Huang, and Lan-Sun Zheng. Carbon arc production of heptagon-containing fullerene [68]. *Nature communications*, 2:ncomms1431, 2011.
- [22] Yukako Ueno and Yoshio Agaoka. Tilings of the 2-dimensional sphere by congruent right triangles. *Memoirs of the Faculty of Integrated Arts and Sciences, Hiroshima University. IV, Science reports: studies of fundamental and environmental sciences*, 22:1–23, 1996.
- [23] Yukako Ueno, Yoshio Agaoka, et al. Classification of tilings of the 2-dimensional sphere by congruent triangles. *Hiroshima Mathematical Journal*, 32(3):463–540, 2002.
- [24] Zhi Wang, Hai-Feng Su, Yuan-Zhi Tan, Stan Schein, Shui-Chao Lin, Wei Liu, Shu-Ao Wang, Wen-Guang Wang, Chen-Ho Tung, Di Sun, et al. Assembly of silver trigons into a buckyball-like ag180 nanocage. *Proceedings of the National Academy of Sciences*, 114(46):12132–12137, 2017.